

High-temperature charge-ordering fluctuation in manganites

K. H. Kim,^{1,*} M. Uehara,^{1,†} and S-W. Cheong^{1,2}

¹*Department of Physics and Astronomy, Rutgers University, Piscataway, New Jersey 08854*

²*Bell Laboratories, Lucent Technologies, Murray Hill, New Jersey 07974*

(Received 30 November 1999)

High-temperature (T) studies of $\text{La}_{1-x}\text{Ca}_x\text{MnO}_3$ show that charge and phonon transport is significantly suppressed in a narrow doping region of $x \approx \frac{1}{2}$ and in a wide T range up to 900 K, which accompanies anomalous broadening of x-ray Bragg peaks. Contrarily, ferromagnetic (FM) correlation above Curie T is sharply enhanced at $x \approx \frac{3}{8}$. All these observations indicate the presence of short-range charge ordering (CO) correlation at high T , possibly in the form of a FM “zigzag,” a small segment of the CE-type CO state. The decoupling and coupling of the FM zigzags for $x \approx \frac{3}{8}$ and $\frac{1}{2}$, respectively, is consistent with our results.

Recent extensive studies have shown that the formation of static or dynamic charge/spin stripes is the generic feature of the doped Mott insulators.¹ The static charge ordering (CO) with stripe correlation has been observed in layered nickelates,² perovskite manganites,³ and doped orthoferrites.⁴ In addition, the presence of the *static* correlation of the charge/spin stripes has been observed in layered cuprates in the region where superconductivity is suppressed.⁵ Furthermore, it has been proposed that the incommensurate inelastic neutron peaks observed in superconducting cuprates are due to the *dynamic* charge/spin stripe correlation.⁶ Therefore, understanding the relationship between the static or dynamic charge/spin stripe correlation with other physical properties such as superconductivity in doped Mott insulators is one of the challenging issues in current condensed matter physics.

In mixed-valent manganites, the orbital degree of freedom associated with Mn^{3+} ions, in addition to charge and spin degrees of freedom, plays an important role. The static charge/orbital ordering with stripe patterns is now well established, especially in $\text{La}_{1-x}\text{Ca}_x\text{MnO}_3$ with $x \geq 0.5$ at a low-temperature (T) region. CO in manganites occurs as periodic arrays of the sheetlike arrangement of Mn^{3+} ions.⁷ In this scheme, the CO state of $\text{La}_{0.5}\text{Ca}_{0.5}\text{MnO}_3$ is special in the sense that the density of $\text{Mn}^{3+}\text{-Mn}^{4+}$ pairs is highest. In $\text{La}_{0.5}\text{Ca}_{0.5}\text{MnO}_3$, all of the charge, orbital, and spin degrees of freedom freeze into the so-called CE-type stable configuration below 180 K (for heating).^{8,9}

Even though static, long-range striped ordering of charge, orbital, and spin degrees of freedom in manganites is well established, the dynamic or short-range correlation of these degrees of freedom is poorly understood. In the simple double exchange (DE) mechanism, hopping of e_g electron of Mn^{3+} induces ferromagnetic (FM) coupling between localized t_{2g} spins.¹⁰ Thus, the FM correlation in $\text{La}_{1-x}\text{Ca}_x\text{MnO}_3$ is supposed to vary as $x(1-x)$, and should be optimized at $x=0.5$, basically because of the maximum number of neighboring $\text{Mn}^{3+}\text{-Mn}^{4+}$ pairs. However, the Curie $T(T_C)$ peaks mysteriously at $x \approx \frac{3}{8}$.⁹ The DE-type FM correlation is, naturally, suppressed by charge localization, which is a prerequisite for CO. Furthermore, superexchange-type magnetic coupling between localized spins sensitively depends on the local orbital configuration, and the orbital degree of freedom can be coupled with the lattice through the Jahn-Teller (JT)

mechanism. Thus, the spatial or temporal fluctuations of charge, spin, orbital, and lattice degrees of freedom ought to be strongly coupled to each other.

In order to reveal the thermal fluctuation nature of these degrees of freedom, we have carefully studied the various physical properties of $\text{La}_{1-x}\text{Ca}_x\text{MnO}_3$ with x near $\frac{1}{2}$ and $\frac{3}{8}$ at high- T regions. Surprisingly, the suppression of electronic conductivity and phononic thermal conductivity exists in a narrow doping range of $x \approx \frac{1}{2}$, which persists up to 900 K, far above static ordering T . On the other hand, we found that FM correlation at room T , above T_C , is sharply optimized at $x \approx \frac{3}{8}$. All of these behaviors can be understood in terms of varying degree of CO correlation with Ca doping level.

High-quality polycrystalline specimens of $\text{La}_{1-x}\text{Ca}_x\text{MnO}_3$ with various x near $\frac{1}{2}$ and $\frac{3}{8}$ have been prepared with the standard solid-state reaction with an identical synthesis condition. Resistivity (ρ) was measured with the standard four-probe method with accurate geometry from 4 to 900 K, and absolute thermal conductivity (κ) was measured from 8 to 310 K with the steady state method (employing a radiation shield). Magnetization (M) was measured by using Quantum Design superconducting quantum interference device (SQUID) magnetometer, and x-ray powder diffraction data were taken by using a Rigaku diffractometer. Magnetization data show that the system with $0.45 \leq x \leq 0.50$ undergoes FM transition at 240–220 K, accompanied by antiferromagnetic (AFM) CO at 160–180 K (for heating).^{9,11} The specimens with x near $\frac{3}{8}$ undergo only FM transition at ≤ 270 K, and CO transition around 200 and 220 K was observed in the $x=0.52$ and 0.55 samples, respectively.

Fig. 1(a) shows the $\rho(T)$ curves for $\text{La}_{1-x}\text{Ca}_x\text{MnO}_3$ with x near 0.5 from 4 to 900 K. First, we discuss the behaviors of ρ with the variation of x at low T . For $x=0.48$, the FM metallic phase is dominant below 220 K even though a short-range CO phase probably coexists as suggested by a broad hump and small hysteresis at 100–180 K.¹² However, with x approaching 0.5 from below, the CO state stabilizes at low T . Thus, ρ near $x=0.5$ at low T increases systematically with x , and shows the insulating T dependence when $x \geq 0.485$. As shown in Fig. 2(a) (open circles), ρ (100 K) shows such a systematic increase with x approaching 0.5 from below, consistent with a crossover from the FM metallic to the CO

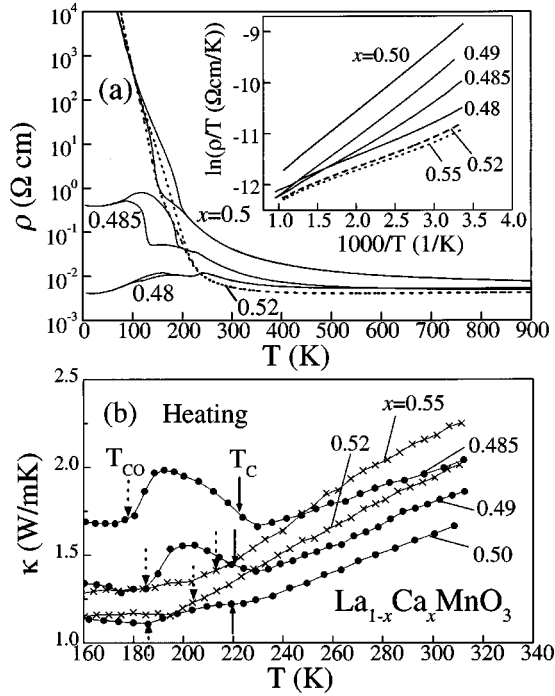


FIG. 1. (a) T -dependent ρ curves (for heating and cooling) of $\text{La}_{1-x}\text{Ca}_x\text{MnO}_3$ near $x=0.5$ from 4 to 900 K. The inset shows $\ln(\rho/T)$ vs $1/T$ curves. (b) $\kappa(T)$ (for heating) for $\text{La}_{1-x}\text{Ca}_x\text{MnO}_3$, $x \approx 0.5$. The solid and dotted arrows show T_C and T_{CO} [determined from $M(T)$ and $\rho(T)$], respectively.

insulating states. Once CO is stabilized at low- T region for $x \geq 0.5$, $\rho(100 \text{ K})$ becomes insensitive on x .

It is intriguing to note that as evident in Fig. 1(a), ρ of $\text{La}_{0.5}\text{Ca}_{0.5}\text{MnO}_3$ at $T > T_{CO}$ is considerably larger than that of any neighboring compositions, and this behavior persists up to 900 K. To unveil this unexpected behavior in detail, we have systematically changed the chemical doping level with fine spacing of x near 0.5. The $\rho(300 \text{ K})$ vs x plot in Fig. 2(a) summarizes the results, showing a clear maximum at $x = 0.5$. Moreover, the $\rho(900 \text{ K})$ vs x plot confirms that the maximum behavior at $x = 0.5$ persists up to, at least, 900 K. A previous study revealed that an adiabatic small polaron model, with $\rho = \rho_0 T \exp(E_a/k_B T)$, describes high- T ρ of $\text{La}_{1-x}\text{Ca}_x\text{MnO}_3$ in broad doping and T ranges ($0 \leq x \leq 1$ and $\sim 300 \text{ K} \leq T \leq 1100 \text{ K}$).¹³ Here, E_a represents the activation energy of small polarons, i.e., the potential barrier that polarons must overcome to hop to the next site. The inset of Fig. 1 shows that $\ln(\rho/T)$ vs $1/T$ plot of our data at high- T region is quite linear, corroborating with the adiabatic small polaron model. Interestingly, E_a is systematically enhanced at $x = 0.5$, as shown in Fig. 2(b). Therefore, the strong charge localization tendency at $x = 0.5$ up to very high T , far above T_{CO} , is closely associated with the enhancement of polaron activation energy.

To gain further insights into understanding this surprising result, we have measured T -dependent κ [Fig. 1(b): heating]. At temperatures above T_C , $\kappa(T)$ for $x < 0.5$ increases linearly with increasing T , which is unusual in crystalline solids. First, we point out that the electronic κ estimated from ρ by using the Wiedemann-Franz law is negligible. It has been known that the electronic κ of adiabatic small polarons is also very small.¹⁴ In addition, an earlier work on FM man-

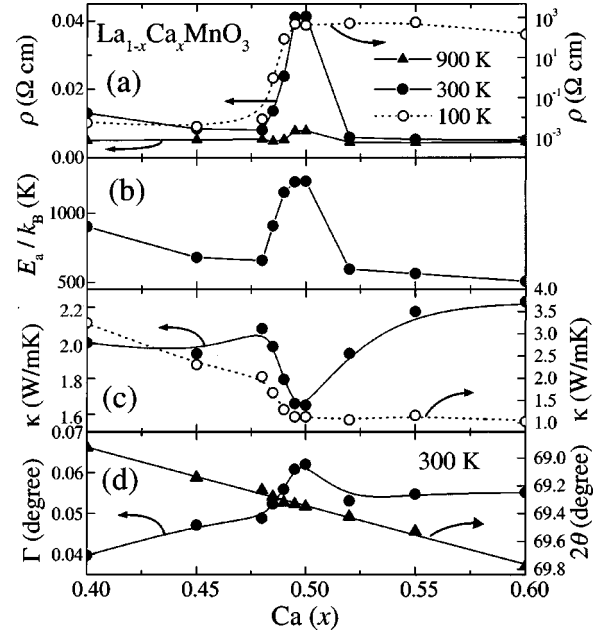


FIG. 2. (a) and (c) ρ and κ values at 100 and 300 K for $\text{La}_{1-x}\text{Ca}_x\text{MnO}_3$ near $x=0.5$, respectively. (b) The activation energy of small polarons, E_a/k_B , vs x plot, obtained from the inset of Fig. 1. (d) The x dependence of the peak width, Γ , and the center position of the (242) x-ray Bragg peak at 300 K, estimated from Gaussian fitting of the data in Fig. 3. The dotted and solid lines are guides for the eyes.

ganites has shown that the anomalous behavior of κ , i.e., a linear increase above T_C is well explained by the phononic κ , coupled with large anharmonic lattice distortions.¹⁵ Thus, it is evident that at a high- T region of $\text{La}_{1-x}\text{Ca}_x\text{MnO}_3$ ($x \approx 0.5$), the electronic contribution to κ is negligible, and the phonon contribution, possibly related to large anharmonic lattice distortions, dominates the measured κ .

The abrupt κ increase near T_C in $\kappa(T)$ of $x = 0.485, 0.49,$ and 0.50 of Fig. 1(b) is due to the reduced lattice distortions in the FM-metallic state, and this κ increase at T_C becomes smaller with x approaching 0.5. For $x \leq 0.5$, κ tends to decrease at T_{CO} , which can be attributed to the large (JT -type) lattice distortion associated with CO. For $x > 0.5$, κ shows only slight slope changes near T_{CO} , as seen in the κ data of $x = 0.52$ and 0.55 . As shown in Fig. 2(c), κ at a low- T region decreases systematically with x approaching 0.5 (due to the stabilization of the CO state), and remains small when $x > 0.5$. We note that even if the κ values of $x = 0.52$ and 0.55 are similar to that of $x = 0.5$ at low T , they become considerably larger than that of $x = 0.5$ for $T > T_{CO}$. This behavior is well illustrated in the $\kappa(300 \text{ K})$ vs x plot [solid circles in Fig. 2(c)], demonstrating a clear minimum at $x = 0.5$. This suppression of $\kappa(300 \text{ K})$ at $x = 0.5$ correlates well with the ρ peaking near 0.5 at 300 K. Therefore, our results in Figs. 1 and 2 show that the lattice thermal conductivity as well as charge transport is suppressed in the high- T region of the half-doped manganite.

Directly related with the suppression of phononic κ , there exists a slight, but noticeable broadening of the x-ray Bragg peaks for $x = 0.5$ at room T . One example of the broadened x-ray peaks is shown in Fig. 3, displaying the compositional change of the (242) Bragg peak (in the orthorhombic $Pbnm$

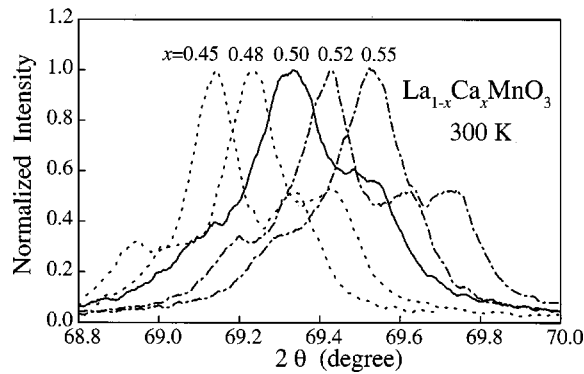


FIG. 3. X-ray intensity profiles of the (242) Bragg peak (center) at 300 K for $\text{La}_{1-x}\text{Ca}_x\text{MnO}_3$ near $x=0.5$.

notation) of x-ray powder diffraction at 300 K. The (242) Bragg peak, centered at $2\theta \approx 69.3^\circ$ for $x=0.5$, changes its position to higher angles as x increases. The left and right sides of the (242) Bragg peak are due to the (004)-(400) peaks and $K\alpha_2$ of the (242) and (004)-(400) peaks, respectively. As evident in Fig. 3, the peak width, Γ , of the central (242) peak is considerably broad at $x=0.5$. To extract the x dependence of Γ , we have fitted the intensity profiles as a sum of three Gaussian peaks [by neglecting the weak $K\alpha_2$ peaks of (004) and (400)]. The solid squares and triangles in Fig. 2(d) represent fitting results for Γ and the center position of the (242) peak, respectively. The center position increases almost linearly with x , indicating the linear lattice contraction with increasing x . On the other hand, Γ shows a clear maximum at $x=0.5$. This broadening of Γ indicates a slight distribution of lattice constants in the half-doped manganite at room T .¹⁶

An early study of synchrotron x-ray scattering for $\text{La}_{0.5}\text{Ca}_{0.5}\text{MnO}_3$ showed a drastic broadening of all the Bragg peaks in the FM region between T_C and T_N ($\approx T_{CO}$).¹⁶ After this discovery, an electron-diffraction study showed that the fine scale (~ 100 Å) coexistence of CO and FM phases is responsible for the drastic broadening of x-ray Bragg peaks.³ What our data in Fig. 3 indicate is that this Bragg peak broadening for $x \approx 0.5$ persists even at room T , far above T_C and T_{CO} . Therefore, the Bragg peak broadening at room T suggests that short-range CO exists in the paramagnetic state of the half-doped manganite. We cannot rule out the possibility of dynamic correlation of CO at room T . The spatial variation of lattice constants, indicated by the Bragg peak broadening, can shorten phonon lifetime, and thus suppresses the phononic κ . The enhancement of ρ up to 900 K in $\text{La}_{0.5}\text{Ca}_{0.5}\text{MnO}_3$ indicates that the spatial or dynamic CO fluctuation probably persists even at T ranges much higher than long-range ordering T .¹⁷ We emphasize that the observed Bragg peak broadening indicates that various anomalous behaviors of $x \approx 0.5$ are *bulk effects*. In other words, the ρ enhancement and the κ suppression at $x \approx 0.5$ are not due to, for example, grain boundaries in our polycrystalline specimens. We also note that our findings are not consistent with La/Ca ionic ordering because the La/Ca ordering should reduce ρ .

Since CO correlation can influence magnetic correlation, we have measured the evolution of magnetic susceptibility ($\chi \equiv M/H$) at room T (above T_C) as a function of x . We

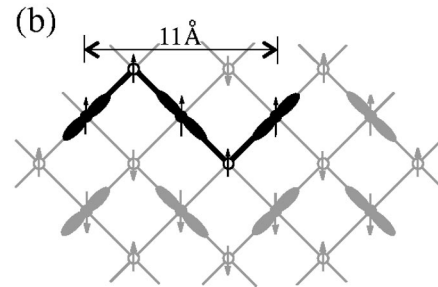
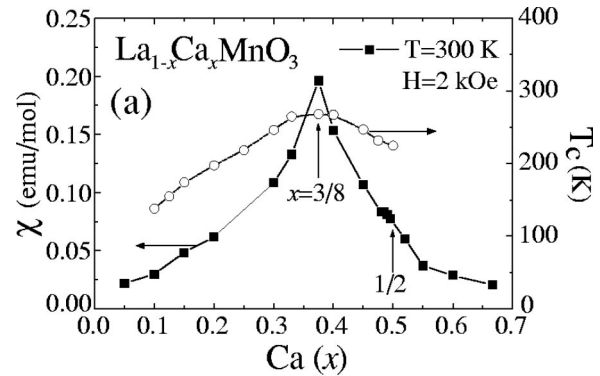


FIG. 4. (a) The x dependence of χ (closed squares) at 300 K (left axis). The open circles show the T_C variation determined from $\chi(T)$ (right axis). (b) A schematic of FM zigzag chains, coupled antiferromagnetically to each other. Open circles are Mn^{4+} and the lobes show the e_g orbitals of Mn^{3+} . A FM zigzag of ~ 11 Å is shown with dark hue.

found a few surprising results as shown in Fig. 4(a). First, we found that $\chi(T)$ above T_C roughly follows the Curie-Weiss law, and the Curie-Weiss T is FM for all x studied. Consistent with earlier results, the T_C vs x plot shows a *broad bump* near $x = \frac{3}{8}$.⁹ On the other hand, $\chi(x)$ at 300 K *sharply peaks* at $x = \frac{3}{8}$. This pronounced peaking of $\chi(x)$ above T_C at the commensurate carrier concentration of $\frac{3}{8}$ suggests an extraordinary possibility; the presence of short-range or dynamic correlation of charge/orbital ordering in such a way as to produce special FM coupling in addition to DE-type FM coupling.

It is important to understand how such short-range charge correlation can promote FM coupling, which is seemingly counterintuitive. In manganites, it has been well established that the CE-type CO is very stable in broad x ranges, at least at low T . For example, the CE-type CO has been commonly observed in $\text{La}_{1-x}\text{Ca}_x\text{MnO}_3$ and $\text{Nd}_{1-x}\text{Sr}_x\text{MnO}_3$ for $x \approx 0.5$. In addition, the CE-type CO has been reported even when x deviates significantly from 0.5. For example, the CE-type CO occurs in $\text{Pr}_{1-x}\text{Ca}_x\text{MnO}_3$ with $0.3 < x \leq 0.5$, and also in $(\text{La}, \text{Pr})_{5/8}\text{Ca}_{3/8}\text{MnO}_3$ at low T .¹² Thus, it is appealing to assume that short-range or dynamic CO at high T of $\text{La}_{1-x}\text{Ca}_x\text{MnO}_3$ ($0.2 < x \leq 0.5$) is also the CE type. In the CE-type CO, there exist FM zigzag chains [Fig. 4(b)], which couple to each other antiferromagnetically.^{8,18,19} It is conceivable that at high T , the CO correlation is so short that the short-range CO state may contain only one short FM zigzag [$\text{Mn}^{3+}\text{-Mn}^{4+}\text{-Mn}^{3+}\text{-Mn}^{4+}\text{-Mn}^{3+}$; shown with dark hue in Fig. 4(b)] with ~ 11 Å in length or one short FM ‘‘zig or zag’’ ($\text{Mn}^{3+}\text{-Mn}^{4+}\text{-Mn}^{3+}$) with ~ 5.5 Å in length. Then, these extended objects can enhance FM correlation overall. The short FM zigzag can be considered as correlated pol-

arons or a ferromagnetic polaron cluster, and may exhibit dynamic nature. Note that the carrier concentration of the short FM zigzag (zig or zag) corresponds to $x=0.4$ ($\frac{1}{3}$), which is close to $x\approx\frac{3}{8}$ for the enhanced FM correlation. However, if the range of CO becomes slightly longer, then the zigzag may couple with the neighboring zigzags antiferromagnetically so that FM correlation can be reduced. This effect can be significant at $x\approx 0.5$ where CO tendency is strong because carrier concentration matches the CE-type ordering.²⁰ This remarkable scenario remains to be confirmed by local probe measurements such as x-ray or neutron-scattering experiments.

In conclusion, we discussed the suppression of electronic conductivity as well as phononic thermal conductivity, and the broadening of Bragg peaks in a narrow composition range near $x=0.5$, but in a very broad T range up to 900 K. On the other hand, FM correlation is strongly enhanced for x near $\frac{3}{8}$ at high T . All these findings can be consistent with spatial or temporal fluctuation of CO at high T . We have

proposed an appealing scenario of the presence of FM zigzags which can be coupled or decoupled, depending on x . The ‘‘decoupled’’ short FM zigzag can enhance the overall FM correlation at x near $\frac{3}{8}$, and the AFM coupling of FM zigzags can progressively increase with x , and be maximized at $x\approx 0.5$ where charge localization tendency is strong. Our work clearly provides a new paradigm for studying the fluctuation nature of CO correlation in various doped Mott insulators, including mixed-valent manganites and superconducting cuprates.

We recently became aware that the neutron-scattering study of $\text{La}_{0.7}\text{Ca}_{0.3}\text{MnO}_3$ by Adams *et al.*²¹ are consistent with our proposed scenario of CO correlation above T_C . They report the presence of the CE-type CO correlation (correlation length of ~ 10 Å) above T_C .

We were partially supported by the NSF-DMR-9802513. K.H.K. and M.U. were partially supported by the KOSEF and by the JPSJ, respectively.

*Present address: Research Institute of Basic Sciences, Seoul National University, Seoul 151-742, Korea.

†Present address: Department of Physics, Aoyama-Gakuin University, Tokyo 157-8572, Japan.

¹V. J. Emery and S. A. Kivelson, *Physica C* **209**, 597 (1993); J. Zaanen, *Science* **286**, 251 (1999).

²T. Katsufuji *et al.*, *Phys. Rev. B* **60**, R5097 (1999), and references therein.

³C. H. Chen and S-W. Cheong, *Phys. Rev. Lett.* **76**, 4042 (1996).

⁴J. Q. Li, Y. Matsui, S. K. Park, and Y. Tokura, *Phys. Rev. Lett.* **79**, 297 (1997).

⁵J. M. Tranquada *et al.*, *Nature (London)* **375**, 561 (1995).

⁶S-W. Cheong *et al.*, *Phys. Rev. Lett.* **67**, 1791 (1991); H. A. Mook *et al.*, *Nature (London)* **395**, 580 (1998).

⁷S. Mori, C. H. Chen, and S-W. Cheong, *Nature (London)* **392**, 473 (1998).

⁸J. B. Goodenough, *Phys. Rev.* **100**, 564 (1955).

⁹S-W. Cheong and C. H. Chen, in *Colossal Magnetoresistance, Charge Ordering and Related Properties of Manganese Oxides*, edited by C. N. R. Rao and B. Raveau (World Scientific, Singapore, 1998).

¹⁰C. Zener, *Phys. Rev.* **82**, 403 (1951); P. W. Anderson and H. Hasegawa, *ibid.* **100**, 675 (1955); P. G. de Gennes, *ibid.* **118**, 141 (1960).

¹¹M. Roy, J. F. Mitchell, A. P. Ramirez, and P. Schiffer, *Phys. Rev. B* **58**, 5185 (1998).

¹²M. Uehara, S. Mori, C. H. Chen, and S-W. Cheong, *Nature (London)* **389**, 560 (1999); K. H. Kim *et al.*, *Phys. Rev. Lett.* **84**, 2961 (2000).

¹³D. C. Worledge, L. Miéville, and T. H. Geball, *Phys. Rev. B* **57**, 15 267 (1998).

¹⁴See, for example, J. L. Cohn *et al.*, *Phys. Rev. B* **56**, R8495 (1997); C. Wood, D. Emin, and P. E. Gray, *ibid.* **31**, 6811 (1985).

¹⁵D. W. Visser, A. P. Ramirez, and M. A. Subramanian, *Phys. Rev. Lett.* **78**, 3947 (1997).

¹⁶P. G. Radaelli *et al.*, *Phys. Rev. Lett.* **75**, 4488 (1995).

¹⁷M. v. Zimmermann *et al.*, *Phys. Rev. Lett.* **83**, 4872 (1999).

¹⁸J. van den Brink, G. Khaliullin, and D. I. Khomskii, *Phys. Rev. Lett.* **83**, 5118 (1999).

¹⁹S. Yunoki, T. Hotta, and E. Dagotto, *Phys. Rev. Lett.* **84**, 3714 (2000).

²⁰We found that, in general, $\rho(300\text{ K})$ for $x<0.5$ (including $x\approx\frac{3}{8}$ where T_C is maximized) is larger than that for $x>0.5$ (including $x\approx\frac{5}{8}$ where T_{CO} is optimized) even though the ground state is metallic (insulating) for $x<(>)0.5$, which corroborates with short-range CO at high T for x near or smaller than 0.5.

²¹C. P. Adams, J. W. Lynn, Y. M. Mukovskii, A. A. Arsenov, and D. A. Shulyatev, *Phys. Rev. Lett.* (to be published).